

# Dirac-like plasmons in honeycomb lattices of metallic nanoparticles

Guillaume Weick,<sup>1</sup> Claire Woollacott,<sup>2</sup> William L. Barnes,<sup>2</sup> Ortwin Hess,<sup>3</sup> and Eros Mariani<sup>2</sup>

<sup>1</sup>*Institut de Physique et Chimie des Matériaux de Strasbourg, Université de Strasbourg,  
CNRS UMR 7504, 23 rue du Loess, BP 43, F-67034 Strasbourg Cedex 2, France*

<sup>2</sup>*Centre for Graphene Science, Department of Physics and Astronomy,  
University of Exeter, Stocker Rd. EX4 4QL Exeter, UK*

<sup>3</sup>*The Blackett Laboratory, Department of Physics, Imperial College London, South Kensington Campus, London SW7 2AZ, UK*

We consider a two-dimensional honeycomb lattice of metallic nanoparticles, each supporting a localized surface plasmon, and study the properties of the collective plasmons resulting from the near field dipolar interaction between the nanoparticles. We analytically investigate the dispersion, the effective Hamiltonian and the eigenstates of the collective plasmons for an arbitrary orientation of the individual dipole moments. When the polarization points close to the normal to the plane the spectrum presents Dirac cones, similar to those present in the electronic band structure of graphene. We show that the corresponding eigenstates of the collective plasmons represent Dirac-like massless bosonic excitations. We further discuss how one can manipulate the Dirac points in the Brillouin zone and open a gap in the collective plasmon dispersion by modifying the polarization of the localized surface plasmons, paving the way for a fully tunable plasmonic analogue of graphene.

PACS numbers: 73.20.Mf, 78.67.Bf, 73.22.Lp, 73.22.Pr

Light has been the source of inspiration for scientific thinking for millennia. Ancient Assyrians developed the first lenses in order to bend the trajectory of light and control its propagation. In contrast to the macroscopic scale, the use of light to observe microscopic structures poses difficulties due to the diffraction limit [1]. In an attempt to overcome this limit and observe subwavelength structures, plasmonic nanostructures have been created [2, 3], like isolated metallic nanoparticles [4]. The evanescent field at the surface of the nanoparticle, associated to the localized surface plasmon (LSP) resonance [5], produces strong optical field enhancement in the subwavelength region, allowing one to overcome the diffraction limit and achieve resolution at the molecular level [6].

While the field of plasmonics mostly focuses on single or few structures, the creation of ordered arrays of nanoparticles constitutes a bridge to the realm of metamaterials. This interesting contamination resulted in plasmonic metamaterials that exhibit unique properties beyond traditional optics, such as negative refractive index [7], perfect lensing [8], the exciting perspective of electromagnetic invisibility cloaking [9], and “trapped rainbow” slow light exploiting the inherent broadband nature of plasmonics [10]. Indeed, in plasmonic metamaterials the interaction between LSPs on individual nanoparticles generates extended plasmonic modes involving all LSPs at once [11, 12]. Understanding the nature and properties of these plasmonic modes [referred to as “collective plasmons” (CPs) in what follows] is of crucial importance as they are the channel guiding electromagnetic radiation with strong lateral confinement over macroscopic distances.

CPs in periodic arrays of metallic nanoparticles are an active area of research in plasmonics because the interaction of the LSP resonances can lead to dramatic changes in the overall optical response of such structures. For example, it was both predicted [13] and observed [14] that the plasmonic response of a periodic array of nanoparticles could be significantly narrowed with respect to the single particle response if the in-

terparticle separation was of the order of the resonant wavelength of the LSP. Further work has shown that these coupled resonances are relevant to applications in light emission. For example, the direction and polarization of light from adjacent fluorescent species can be controlled using such arrays [15]. The extended nature of the collective resonances means that there is scope for harvesting emission from sources spread over large volumes. Arrays of metallic nanoparticles may be designed to exhibit stop-gaps and band-edges [16] and are also being intensively investigated in the context of light harvesting for photovoltaic devices [17].

The dispersion of CPs and their physical nature crucially depend on the lattice structure of the metamaterial and on the microscopic interaction between LSPs. A lattice which recently generated remarkable interest in the condensed matter community is the honeycomb structure exhibited by graphene, a two-dimensional (2D) monolayer of carbon atoms [18]. In the case of graphene, the hopping of electrons between neighboring atoms gives rise to a rich band structure characterized by the presence of fermionic massless Dirac quasiparticles close to zero energy [19]. The chirality associated with pseudo-relativistic Dirac fermions results in several of the remarkable properties of graphene, such as a nontrivial Berry phase accumulated in parallel transport [20] and the suppression of electronic backscattering from smooth scatterers [21], which is ultimately responsible for the very high mobility of graphene samples. Undoubtedly, it would be exciting to harvest the remarkable physical properties of electrons in graphene in suitably designed plasmonic metamaterials (“plasmonic graphene”) by analyzing the Hamiltonian and the consequent nature of CP eigenmodes in 2D honeycomb lattices of metallic nanoparticles. This is the purpose of the present theoretical paper.

We analytically show how the problem of interacting LSPs in the honeycomb structure can be mapped to the kinetic problem of electrons hopping in graphene, yielding massless

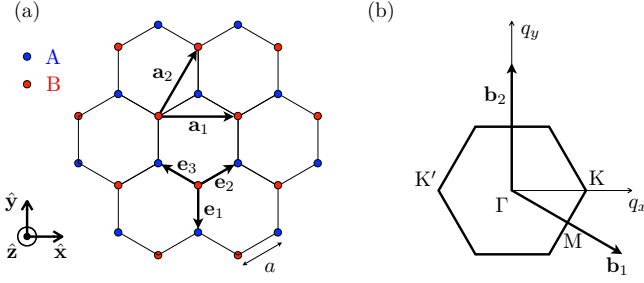


FIG. 1. (color online). (a) Honeycomb lattice with lattice constant  $a$  and lattice vectors  $\mathbf{a}_1 = a(\sqrt{3}/2, 0)$  and  $\mathbf{a}_2 = a(\sqrt{3}/2, 3/2)$ . The three vectors  $\mathbf{e}_1 = a(0, -1)$ ,  $\mathbf{e}_2 = a(\sqrt{3}/2, 1/2)$  and  $\mathbf{e}_3 = a(-\sqrt{3}/2, 1/2)$  connect the A and B inequivalent lattice sites (blue/light gray and red/dark gray dots in the figure). (b) First Brillouin zone in reciprocal space with primitive vectors  $\mathbf{b}_1 = \frac{2\pi}{3a}(\sqrt{3}, -1)$  and  $\mathbf{b}_2 = \frac{4\pi}{3a}(0, 1)$ .

Dirac-like bosonic CPs in the vicinity of two Dirac points in the Brillouin zone. While the conical dispersion of plasmons in a honeycomb lattice of nanoparticles has been discussed in the past for out-of-plane or purely in-plane polarization [22], here we unveil the *full Hamiltonian* of quantum CPs as well as the pseudospin structure of the CP eigenmodes for dipolar LSPs with *arbitrary* orientation. The existence of Dirac points is robust for a small in-plane component of the polarization, where the system maps to strained graphene [23], while band gaps can emerge for increasing in-plane polarization. At energies away from the Dirac point, van Hove singularities [24] emerge in the CP density of states (DOS), associated with Lifshitz transitions in the topology of equipotential lines [25]. Our analysis highlights the physical nature of CP eigenmodes as well as the tunability of their band structure and of the corresponding DOS with the polarization of light, which can be crucial for enhancing the coupling of light with the plasmonic metamaterial at different wavelengths.

Specifically, we consider an ensemble of identical spherical metallic nanoparticles of radius  $r$  forming a 2D honeycomb lattice with lattice constant  $a$  embedded in a dielectric medium with dielectric constant  $\epsilon_m$  (see Fig. 1). The nanoparticles are located at positions  $\mathbf{R}_s$ , with  $s = A, B$  a sublattice index which distinguishes the inequivalent lattice sites. Each individual nanoparticle supports a LSP resonance which can be triggered by an oscillating external electric field with wavelength  $\lambda$  much larger than  $r$ . Under such a condition, the LSP is a dipolar collective electronic excitation at the Mie frequency  $\omega_0 = \omega_p / \sqrt{1 + 2\epsilon_m}$ , which typically lies in the visible or near-infrared part of the spectrum [5]. Here,  $\omega_p = \sqrt{4\pi n_e e^2 / m_e}$  is the plasma frequency, with  $n_e$ ,  $-e$  and  $m_e$  the electron density, charge, and mass, respectively. The LSP corresponding to the electronic center-of-mass excitation can be generally considered as a quantum bosonic mode, particularly when the size of the nanoparticle is such that quantization effects are important [26–29]. The noninteracting part of the Hamiltonian describing the independent LSPs on the

honeycomb lattice sites reads [27, 28]

$$H_0 = \sum_{s=A,B} \sum_{\mathbf{R}_s} \left[ \frac{\Pi_s^2(\mathbf{R}_s)}{2M} + \frac{M}{2} \omega_0^2 h_s^2(\mathbf{R}_s) \right], \quad (1)$$

where  $h_s(\mathbf{R})$  is the displacement field associated with the electronic center of mass at position  $\mathbf{R}$ ,  $\Pi_s(\mathbf{R})$  its conjugated momentum and  $M = N_e m_e$  its mass, with  $N_e$  the number of valence electrons in each nanoparticle.

The nature of the coupling between LSPs in different nanoparticles depends on their size and distance. Provided that the wavelength associated with each LSP is much larger than the interparticle distance  $a$  and that  $r \lesssim a/3$  [12], each LSP can be considered as a point dipole with dipole moment  $\mathbf{p} = -eN_e h_s(\mathbf{R}) \hat{\mathbf{p}}$  which interacts with the neighboring ones through dipole-dipole interaction. Moreover, it has been numerically shown [22] that a quasistatic approximation which only takes into account the near field generated by each dipole qualitatively reproduces the results of more sophisticated simulations in which retardation effects are included. Within such a quasistatic approximation, the interaction between two dipoles  $\mathbf{p}$  and  $\mathbf{p}'$  located at  $\mathbf{R}$  and  $\mathbf{R}'$ , respectively, reads [30]  $\mathcal{V} = [\mathbf{p} \cdot \mathbf{p}' - 3(\mathbf{p} \cdot \mathbf{n})(\mathbf{p}' \cdot \mathbf{n})] / \epsilon_m |\mathbf{R} - \mathbf{R}'|^3$  with  $\mathbf{n} = (\mathbf{R} - \mathbf{R}') / |\mathbf{R} - \mathbf{R}'|$ . In what follows, we assume that in a CP eigenmode all nanoparticles are initially polarized in the same direction  $\hat{\mathbf{p}} = \sin \theta (\sin \varphi \hat{\mathbf{x}} - \cos \varphi \hat{\mathbf{y}}) + \cos \theta \hat{\mathbf{z}}$ , where  $\theta$  is the angle between  $\hat{\mathbf{p}}$  and  $\hat{\mathbf{z}}$ , and  $\varphi$  the angle between the projection of  $\hat{\mathbf{p}}$  in the  $xy$  plane and  $\mathbf{e}_1$  [see Fig. 1(a)]. We thus write the total Hamiltonian of our system of coupled LSPs as  $H = H_0 + H_{\text{int}}$ , where  $H_0$  is defined in Eq. (1) and where the dipole-dipole interaction term reads

$$H_{\text{int}} = \frac{(eN_e)^2}{\epsilon_m a^3} \sum_{\mathbf{R}_B} \sum_{j=1}^3 \mathcal{C}_j h_B(\mathbf{R}_B) h_A(\mathbf{R}_B + \mathbf{e}_j). \quad (2)$$

Here,  $\mathcal{C}_j = 1 - 3 \sin^2 \theta \cos^2 (\varphi - 2\pi[j-1]/3)$ , and the vectors  $\mathbf{e}_j$  connect the A and B sublattices [see Fig. 1(a)]. Notice that in Eq. (2), we have only considered the dipole-dipole interaction between nearest neighbors, as the effect of interactions beyond nearest neighbors does not qualitatively change the plasmonic spectrum [31].

The analogy between the plasmonic structure of Fig. 1 and the electronic properties of graphene becomes transparent by introducing the bosonic ladder operators  $a_{\mathbf{R}} | b_{\mathbf{R}} = (M\omega_0/2\hbar)^{1/2} h_{A|B}(\mathbf{R}) + i\Pi_{A|B}(\mathbf{R}) / (2\hbar M\omega_0)^{1/2}$  which satisfy the commutation relations  $[a_{\mathbf{R}}, a_{\mathbf{R}'}^\dagger] = [b_{\mathbf{R}}, b_{\mathbf{R}'}^\dagger] = \delta_{\mathbf{R}, \mathbf{R}'}$  and  $[a_{\mathbf{R}}, b_{\mathbf{R}'}^\dagger] = 0$ . As we will show in the following, the introduction of such operators not only gives access to the plasmon dispersion (which can be calculated classically as well [31]), but also unveils the Dirac nature of the CP quantum states. The harmonic Hamiltonian (1) can be written in terms of the above-mentioned bosonic operators as  $H_0 = \hbar\omega_0 \sum_{\mathbf{R}_A} a_{\mathbf{R}_A}^\dagger a_{\mathbf{R}_A} + \hbar\omega_0 \sum_{\mathbf{R}_B} b_{\mathbf{R}_B}^\dagger b_{\mathbf{R}_B}$ , while Eq. (2) transforms into

$$H_{\text{int}} = \hbar\Omega \sum_{\mathbf{R}_B} \sum_{j=1}^3 \mathcal{C}_j b_{\mathbf{R}_B}^\dagger \left( a_{\mathbf{R}_B + \mathbf{e}_j} + a_{\mathbf{R}_B + \mathbf{e}_j}^\dagger \right) + \text{H.c.} \quad (3)$$

In Eq. (3),  $\Omega = \omega_0(r/a)^3(1 + 2\epsilon_m)/6\epsilon_m$ , such that  $\Omega \ll \omega_0$ . The first term on the right-hand side of Eq. (3) (together with its hermitian conjugate) resembles the electronic tight-binding Hamiltonian of graphene [19], except for three major differences: (i) The Hamiltonian of graphene describes fermionic particles (electrons), while we deal here with *bosonic* excitations (LSPs). (ii) In graphene, an electron “hops” from one lattice site to a neighboring one, i.e., the underlying mechanism linking the two inequivalent sublattices is purely kinetic. In the present case, the mechanism coupling the two sublattices is purely induced by near-field (dipolar) *interactions*, leading to the creation of an LSP excitation at lattice site  $\mathbf{R}_B$  and the annihilation of another LSP at a nearest neighbor located at  $\mathbf{R}_B + \mathbf{e}_j$ . (iii) In (unstrained) graphene, the hopping matrix element between two neighboring atoms is the same for all three bonds, while in our case, the three energy scales  $\hbar\Omega C_j$  ( $j = 1, 2, 3$ ) are in general different and can be tuned by the direction of the polarization  $\hat{\mathbf{p}}$  of the CP eigenmode [cf. Eq. (2)]. For  $0 < \theta \leq \theta_0$  and  $\pi - \theta_0 \leq \theta < \pi$  with  $\theta_0 = \arcsin \sqrt{1/3}$ , the coefficients  $C_j$  are all positive for any  $\varphi$  and have different values, resulting in different couplings between the bonds, thus mimicking the effect of strain in the lattice [23]. For  $\theta_0 < \theta < \pi - \theta_0$ , the signs of the coefficients  $C_j$  depend on  $\varphi$ , and the analogy with strained graphene is no longer valid. In the special case where  $C_1 = C_2 = C_3$  (for  $\theta = 0$  or  $\pi$ ), we expect the CP spectrum to resemble that of the electronic band structure in graphene, since the Bloch theorem does not depend on the quantum statistics of the particles one considers, but only on the structure of the periodic lattice [32]. As we will now show, two slight differences appear in the CP dispersion as compared to the graphene band structure, i.e., the effect of the Hamiltonian  $H_0$  is to produce a global energy shift (by an amount  $\hbar\omega_0$ ), while the “anomalous” term  $\propto b_{\mathbf{R}_B}^\dagger a_{\mathbf{R}_B+\mathbf{e}_j}^\dagger$  in Eq. (3) introduces corrections of order  $(\Omega/\omega_0)^2$  to the spectrum.

Introducing the bosonic operators in momentum space  $a_{\mathbf{q}}$  and  $b_{\mathbf{q}}$  through the Fourier decompositions  $a_{\mathbf{R}}|b_{\mathbf{R}} = \mathcal{N}^{-1/2} \sum_{\mathbf{q}=(q_x, q_y)} \exp(i\mathbf{q} \cdot \mathbf{R}) a_{\mathbf{q}}|b_{\mathbf{q}}$ , with  $\mathcal{N}$  the number of unit cells of the honeycomb lattice, the Hamiltonian  $H = H_0 + H_{\text{int}}$  transforms into  $H = \hbar\omega_0 \sum_{\mathbf{q}} (a_{\mathbf{q}}^\dagger a_{\mathbf{q}} + b_{\mathbf{q}}^\dagger b_{\mathbf{q}}) + \hbar\Omega \sum_{\mathbf{q}} [f_{\mathbf{q}} b_{\mathbf{q}}^\dagger (a_{\mathbf{q}} + a_{-\mathbf{q}}^\dagger) + \text{H.c.}]$  with  $f_{\mathbf{q}} = \sum_{j=1}^3 C_j \exp(i\mathbf{q} \cdot \mathbf{e}_j)$ . The latter Hamiltonian is diagonalized by two successive Bogoliubov transformations [33]. First, we introduce the two bosonic operators

$$\alpha_{\mathbf{q}}^\pm = \frac{1}{\sqrt{2}} \left( \frac{f_{\mathbf{q}}}{|f_{\mathbf{q}}|} a_{\mathbf{q}} \pm b_{\mathbf{q}} \right) \quad (4)$$

in terms of which we obtain  $H = \sum_{\tau=\pm} \sum_{\mathbf{q}} [(\hbar\omega_0 + \tau \hbar\Omega |f_{\mathbf{q}}|) \alpha_{\mathbf{q}}^\tau \alpha_{\mathbf{q}}^\tau + \tau \frac{\hbar\Omega |f_{\mathbf{q}}|}{2} (\alpha_{\mathbf{q}}^\tau \alpha_{-\mathbf{q}}^\tau + \text{H.c.})]$ . Second, we define two new bosonic modes  $\beta_{\mathbf{q}}^\pm = \cosh \vartheta_{\mathbf{q}}^\pm \alpha_{\mathbf{q}}^\pm - \sinh \vartheta_{\mathbf{q}}^\pm \alpha_{-\mathbf{q}}^\pm$ , with  $\cosh \vartheta_{\mathbf{q}}^\pm = 2^{-1/2} [(1 \pm \Omega |f_{\mathbf{q}}|/\omega_0)/(1 \pm 2\Omega |f_{\mathbf{q}}|/\omega_0)^{1/2} + 1]^{1/2}$  and  $\sinh \vartheta_{\mathbf{q}}^\pm = \mp 2^{-1/2} [(1 \pm \Omega |f_{\mathbf{q}}|/\omega_0)/(1 \pm 2\Omega |f_{\mathbf{q}}|/\omega_0)^{1/2} - 1]^{1/2}$ , which diagonalize the Hamiltonian  $H$  as

$H = \sum_{\tau=\pm} \sum_{\mathbf{q}} \hbar\omega_{\mathbf{q}}^\tau \beta_{\mathbf{q}}^\tau \beta_{\mathbf{q}}^\tau$ . The two CP branches have dispersions

$$\omega_{\mathbf{q}}^\pm = \omega_0 \sqrt{1 \pm 2 \frac{\Omega}{\omega_0} |f_{\mathbf{q}}|} \quad (5)$$

which reduce to  $\omega_{\mathbf{q}}^\pm \simeq \omega_0 \pm \Omega |f_{\mathbf{q}}|$  to first order in  $\Omega/\omega_0 \ll 1$ , for which we have  $\beta_{\mathbf{q}}^\pm \simeq \alpha_{\mathbf{q}}^\pm$ . Notice that the dispersion (5) can also be obtained classically by normal mode analysis [31].

The dispersion (5) is shown in Fig. 2 in the case of a polarization  $\hat{\mathbf{p}}$  perpendicular to the plane of the honeycomb lattice [ $\theta = 0$ , Fig. 2(a)], in the case of an in-plane polarization [ $\theta = \pi/2$ ,  $\varphi = 0$ , Fig. 2(b)], and for the special case  $\theta = \arcsin \sqrt{1/3}$ ,  $\varphi = 0$  [Fig. 2(c)]. In the first case [Fig. 2(a)], we have gapless modes with two inequivalent Dirac cones centered at the K and K' points located at  $\pm \mathbf{K} = \frac{4\pi}{3\sqrt{3}a}(\pm 1, 0)$  in the first Brillouin zone [cf. Fig. 1(b)], while in the second case, the modes are gapped [Fig. 2(b)]. The dispersion shown in Fig. 2(c) corresponds to a polarization for which  $C_1 = 0$  in Eq. (2), i.e., the bonds linked by  $\mathbf{e}_1$  [cf. Fig. 1(a)] are ineffective and the system is effectively translationally invariant along one direction. Hence, the CP dispersion in Fig. 2(c) does not depend on  $q_y$  and presents Dirac “lines”.

The analogy between the dispersion shown in Fig. 2(a) and the electronic band structure of graphene [19] is striking. Close to the two inequivalent Dirac points K and K' [see Fig. 1(b)], the function  $f_{\mathbf{q}}$  expands as  $f_{\mathbf{q}} \simeq \frac{3a}{2}(\mp \delta q_x + i\delta q_y)$  with  $\mathbf{q} = \pm \mathbf{K} + \delta \mathbf{q}$  ( $|\delta \mathbf{q}| \ll |\pm \mathbf{K}|$ ), such that the dispersion (5) is linear and forms a Dirac cone,  $\omega_{\mathbf{q}}^\pm \simeq \omega_0 \pm v|\delta \mathbf{q}|$ , with group velocity  $v = 3\Omega a/2$ . This feature is consistent with numerical analysis [22]. In the case of graphene, the purely kinetic Hamiltonian is  $H = -t \sum_{\mathbf{q}} f_{\mathbf{q}} b_{\mathbf{q}}^\dagger a_{\mathbf{q}} + \text{H.c.}$ , with  $a_{\mathbf{q}}$  and  $b_{\mathbf{q}}$  fermionic operators, and  $t$  the nearest-neighbor hopping energy (in the case of unstrained graphene, all coefficients  $C_j$  are equal to one in the function  $f_{\mathbf{q}}$ ). The consequent diagonal Hamiltonian  $H = -\sum_{\tau,\mathbf{q}} \tau t |f_{\mathbf{q}}| \alpha_{\mathbf{q}}^\tau \alpha_{\mathbf{q}}^\tau$  is associated with the very same eigenstates  $\alpha_{\mathbf{q}}^\tau$  as in Eq. (4), where the amplitudes of sublattice A and B are linked by  $\pm f_{\mathbf{q}}/|f_{\mathbf{q}}|$ . In the vicinity of the Dirac point K (K'), the Hamiltonian in the AB basis is expanded as  $H = \hbar v \boldsymbol{\sigma} \cdot \delta \mathbf{q}$  ( $H = \hbar v \boldsymbol{\sigma}^* \cdot \delta \mathbf{q}$ ) with  $\boldsymbol{\sigma}$  the vector of Pauli matrices. This massless Dirac Hamiltonian is fulfilled also by CPs near the Dirac points (up to a global energy shift of  $\hbar\omega_0$ ) and the corresponding states are characterized by chirality  $\boldsymbol{\sigma} \cdot \hat{\delta \mathbf{q}} = \pm 1$ . As a consequence, CPs will show similar effects to electrons in graphene like a Berry phase of  $\pi$  [20] and the absence of backscattering off inhomogeneities [21]. This could have crucial implications for the efficient plasmonic propagation in array-based metamaterials.

In Fig. 2, the panels (d)–(f) show the density of states (DOS) corresponding to the spectrum illustrated in the panels (a)–(c). It is interesting to notice the tunability of the DOS with the direction of the polarization, as well as the emergence of van Hove singularities [24]. The latter are associated with Lifshitz transitions [25] in the topology of equipotential lines that percolate at specific energies. The tunability of van Hove

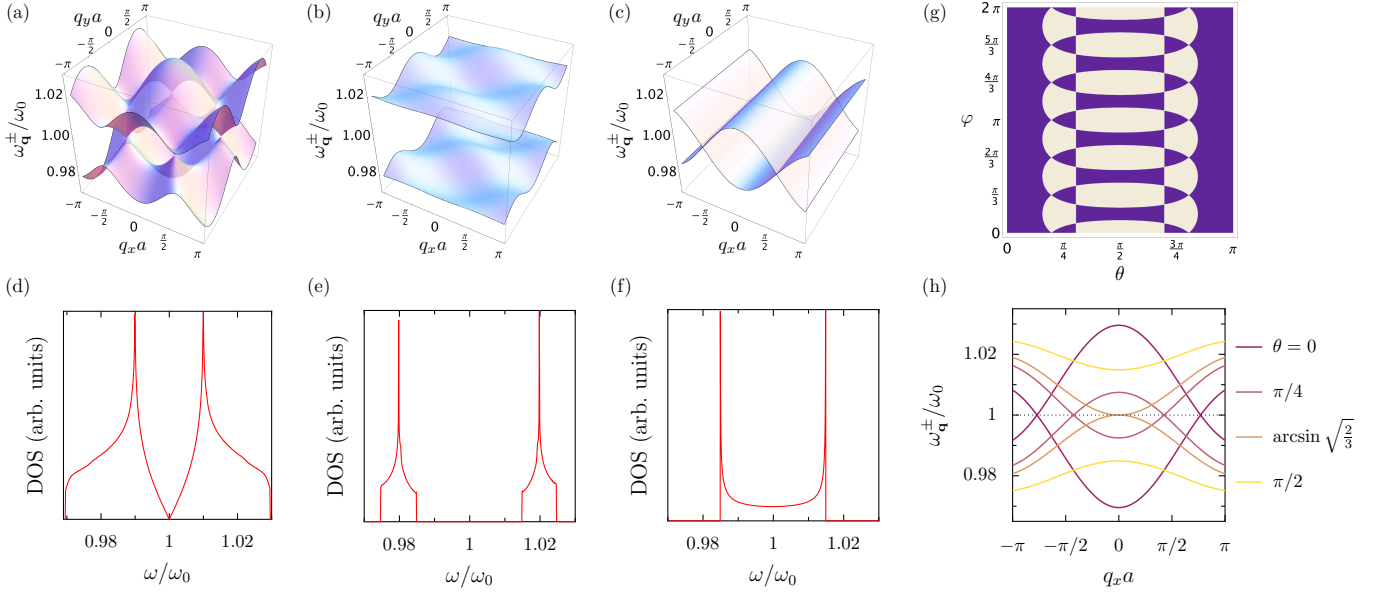


FIG. 2. (color online). (a)–(c) Collective plasmon dispersion relation from Eq. (5) and (d)–(f) corresponding density of states for (a),(d) the out-of-plane mode ( $\theta = 0$ ), (b),(e) one in-plane mode ( $\theta = \pi/2$ ), and (c),(f)  $\theta = \arcsin \sqrt{1/3}$ . (g) Polarization angles ( $\theta, \varphi$ ) for which the collective plasmon dispersion is gapless (dark blue regions) and gapped (white regions). (h) Collective plasmon dispersion along the K'TK direction ( $q_y = 0$ ) for different orientations  $\theta$  of the dipoles. In the figure,  $\varphi = 0$  and  $\Omega/\omega_0 = 0.01$ .

singularities in the spectrum could be of crucial importance to increase the coupling of light of different wavelengths with extended CP modes.

For an arbitrary polarization of the LSPs, we can determine if the CP dispersion is gapless by imposing  $|f_q| = 0$  in Eq. (5), which leads to the condition  $0 \leq [(C_2 + C_3)^2 - C_1^2]/4C_2C_3 \leq 1$  for having gapless plasmonic modes [31]. In Fig. 2(g), we show in dark blue the regions of stability of a massless Dirac spectrum in the  $(\theta, \varphi)$  parameter space for which one has gapless plasmon modes, an example of which is shown in Fig. 2(a). In Fig. 2(g), the white regions correspond to polarizations for which the CP dispersion is gapped [as an example, see Fig. 2(b)]. Thus, changing the polarization allows one to *qualitatively* change the CP spectrum. This is further illustrated in Fig. 2(h) where we show the CP dispersion (5) along the K'TK direction [see Fig. 1(b)] for different angles  $\theta$  of the polarization (in the figure,  $\varphi = 0$ ). As one can see from Fig. 2(h), the two inequivalent Dirac points located at K and K' for  $\theta = 0$  drift as one increases  $\theta$  and they merge at  $\mathbf{q} = 0$  for  $\theta = \arcsin \sqrt{2/3}$ , forming parabolic bands, to finally open a gap for  $\theta > \arcsin \sqrt{2/3}$  (exemplified by  $\theta = \pi/2$  in the figure).

A limitation on the experimental observability of the CP dispersion is plasmonic damping, which tends to blur the resonance frequencies. In order to estimate the feasibility of such experiments, we compare the bandwidth of the CP dispersion to the losses in individual nanoparticles. In the latter, two main sources of dissipation arise: (i) radiation damping with decay rate  $\gamma_{\text{rad}} = 2r^3\omega_0^4/3c^3$  [34] ( $c$  is the speed of light) which dominates for larger nanoparticle sizes, and (ii) Landau damping with decay rate  $\gamma_L = 3v_F g/4r$  [26, 28]

[ $v_F = \hbar(3\pi^2 n_e)^{1/3}/m_e$  is the Fermi velocity and  $g$  a constant of the order of one] which dominates for smaller sizes. Hence, there exists an optimal size  $r_{\text{opt}} = (3v_F g c^3/8)^{1/4}/\omega_0$  for which the total damping  $\gamma_{\text{tot}} = \gamma_{\text{rad}} + \gamma_L$  is minimal. For Ag nanoparticles, we find  $r_{\text{opt}} = 8$  nm for which  $\gamma_{\text{tot}} = 0.1$  eV/ $\hbar$ . Note that in Ag, the interband transitions are decoupled from the LSP, contrary to the case of Au which shows a significantly broader resonance [35]. With an interparticle distance  $a = 3r_{\text{opt}}$  which maximizes the dipolar coupling between nanoparticles [12], we find for Ag that the bandwidth (for  $\epsilon_m = 1$ , and for the out-of-plane polarization) is of the order of  $\Delta\omega = \omega_0^+ - \omega_0^- = \omega_0/9 = 0.6$  eV/ $\hbar$  at the center of the Brillouin zone. Thus  $\Delta\omega$  is sufficiently large when compared to  $\gamma_{\text{tot}}$  that the plasmon excitation is well defined and hence clearly measurable. We expect this to be true even in the presence of inhomogeneous broadening resulting from the size dispersion of the nanoparticles. Moreover, the appropriate use of active (gain-enhanced) media [36] might increase the observability of the CP dispersion and open the way towards a new class of Dirac-point lasing.

A last comment is in order about the excitation of CPs by external photons, whose in-plane momentum must match the plasmonic one. In fact, the vicinity of the Dirac points typically lies outside the light cone. In order to overcome this momentum mismatch and observe the Dirac-like plasmons, one might add an extra periodic modulation of the lattice to allow grating coupling between the incident light and the desired collective modes [3]. Another alternative might be to use a non-linear technique to overcome the momentum mismatch [37].

In conclusion, we demonstrated the strong analogies be-



tween the physical properties of electrons in graphene and those of collective plasmon modes in a 2D honeycomb lattice of metallic nanoparticles. While we considered spherical nanoparticles, our results also extend in principle to arbitrary shapes provided they support dipolar excitations. Whereas the electronic states of graphene can be described by massless Dirac fermions, the CP eigenstates correspond to massless Dirac-like bosonic excitations. The spectrum of the latter can be fully tuned by the polarization of an external light field, opening exciting new possibilities for controlling the propagation of electromagnetic radiation with subwavelength lateral confinement in plasmonic metamaterials.

We thank Cosimo Gorini, Rodolfo Jalabert, and Dietmar Weinmann for stimulating discussions.

- 
- [1] E. Abbe, *Archiv für Mikroskopische Anatomie* **9**, 413 (1873); M. Born and E. Wolf, *Principles of Optics* (Cambridge University Press, Cambridge, 2002).
  - [2] W. L. Barnes, A. Dereux, and T. W. Ebbesen, *Nature* **424**, 824 (2003).
  - [3] S. A. Maier, *Plasmonics: Fundamentals and Applications* (Springer-Verlag, Berlin, 2007).
  - [4] T. Klar, M. Perner, S. Grosse, G. von Plessen, W. Spirkel, and J. Feldmann, *Phys. Rev. Lett.* **80**, 4249 (1998).
  - [5] G. Mie, *Ann. Phys. (Leipzig)* **25**, 377 (1908); U. Kreibig and M. Vollmer, *Optical Properties of Metal Clusters* (Springer-Verlag, Berlin, 1995).
  - [6] K. Kneipp, Y. Wang, H. Kneipp, L. T. Perelman, I. Itzkan, R. R. Dasari, and M. S. Feld, *Phys. Rev. Lett.* **78**, 1667 (1997).
  - [7] V. G. Veselago, *Sov. Phys. Usp.* **10**, 509 (1968); D. R. Smith, W. J. Padilla, D. C. Vier, S. C. Nemat-Nasser, and S. Schultz, *Phys. Rev. Lett.* **84**, 4184 (2000); R. A. Shelby, D. R. Smith, and S. Schultz, *Science* **292**, 77 (2001).
  - [8] J. B. Pendry, *Phys. Rev. Lett.* **85**, 3966 (2000); N. Fang, H. Lee, C. Sun, and X. Zhang, *Science* **308**, 534 (2005).
  - [9] U. Leonhardt, *Science* **312**, 1777 (2006); J. B. Pendry, D. Schurig, and D. R. Smith, *Science* **312**, 1780 (2006); D. Schurig, J. J. Mock, B. J. Justice, S. A. Cummer, J. B. Pendry, A. F. Starr, and D. R. Smith, *Science* **314**, 977 (2006).
  - [10] K. L. Tsakmakidis, A. D. Boardman, and O. Hess, *Nature* **450**, 397 (2007).
  - [11] M. Quinten, A. Leitner, J. R. Krenn, and F. R. Aussenegg, *Opt. Lett.* **23**, 1331 (1998); J. R. Krenn, A. Dereux, J. C. Weeber, E. Bourillot, Y. Lacroute, J. P. Goudonnet, G. Schider, W. Gotschy, A. Leitner, F. R. Aussenegg, and C. Girard, *Phys. Rev. Lett.* **82**, 2590 (1999); S. A. Maier, M. L. Brongersma, P. G. Kik, and H. A. Atwater, *Phys. Rev. B* **65**, 193408 (2002); S. A. Maier, P. G. Kik, H. A. Atwater, S. Meltzer, E. Harel, B. E. Koel, and A. A. G. Requicha, *Nature Mater.* **2**, 229 (2003).
  - [12] M. L. Brongersma, J. W. Hartman, and H. A. Atwater, *Phys. Rev. B* **62**, R16356 (2000); S. Y. Park and D. Stroud, *Phys. Rev. B* **69**, 125418 (2004).
  - [13] K. T. Carron, W. Fluhr, M. Meier, A. Wokaun, and H. W. Lehmann, *J. Opt. Soc. Am. B* **3**, 430 (1986); S. Zou, N. Janel, and G. C. Schatz, *J. Chem. Phys.* **120**, 10871 (2004).
  - [14] V. G. Kravets, F. Schedin, and A. N. Grigorenko, *Phys. Rev. Lett.* **101**, 087403 (2008); B. Auguié and W. L. Barnes, *Phys. Rev. Lett.* **101**, 143902 (2008); Y. Chu, E. Schonbrun, T. Yang, and K. B. Crozier, *Appl. Phys. Lett.* **93**, 181108 (2008).
  - [15] S. R. K. Rodriguez, G. Lozano, M. A. Verschuuren, R. Gomes, K. Lambert, B. De Geyter, A. Hassinen, D. Van Thourhout, Z. Hens, and J. Gómez Rivas, *Appl. Phys. Lett.* **100**, 111103 (2012).
  - [16] S. R. K. Rodriguez, A. Abass, B. Maes, O. T. A. Janssen, G. Vecchi, and J. Gómez Rivas, *Phys. Rev. X* **1**, 021019 (2011).
  - [17] H. A. Atwater and A. Polman, *Nature Mater.* **9**, 205 (2010).
  - [18] K. S. Novoselov, A. K. Geim, S. V. Morozov, D. Jiang, Y. Zhang, S. V. Dubonos, I. V. Grigorieva, and A. A. Firsov, *Science* **306**, 666 (2004).
  - [19] P. R. Wallace, *Phys. Rev.* **71**, 622 (1947); A. H. Castro Neto, F. Guinea, N. M. R. Peres, K. S. Novoselov, and A. K. Geim, *Rev. Mod. Phys.* **81**, 109 (2009).
  - [20] K. S. Novoselov, A. K. Geim, S. M. Morozov, D. Jiang, M. I. Katsnelson, I. V. Grigorieva, S. V. Dubonos, and A. A. Firsov, *Nature* **438**, 197 (2005); Y. Zhang, Y.-W. Tan, H. L. Stormer, and P. Kim, *Nature* **438**, 201 (2005).
  - [21] V. V. Cheianov and V. I. Fal'ko, *Phys. Rev. B*, **74**, 041403(R) (2006).
  - [22] D. Han, Y. Lai, J. Zi, Z.-Q. Zhang, and C. T. Chan, *Phys. Rev. Lett.* **102**, 123904 (2009).
  - [23] L. M. Woods and G. D. Mahan, *Phys. Rev. B* **61**, 10651 (2000); H. Suzuura and T. Ando, *Phys. Rev. B* **65**, 235412 (2002).
  - [24] L. van Hove, *Phys. Rev.* **89**, 1189 (1953).
  - [25] I. M. Lifshitz, *Sov. Phys. JETP* **21**, 1130 (1960).
  - [26] A. Kawabata and R. Kubo, *J. Phys. Soc. Jpn.* **21**, 1765 (1966); C. Yannouleas and R. A. Broglia, *Ann. Phys. (NY)* **217**, 105 (1992); R. A. Molina, D. Weinmann, and R. A. Jalabert, *Phys. Rev. B* **65**, 155427 (2002).
  - [27] L. G. Gerchikov, C. Guet, and A. N. Ipatov, *Phys. Rev. A* **66**, 053202 (2002).
  - [28] G. Weick, R. A. Molina, D. Weinmann, and R. A. Jalabert, *Phys. Rev. B* **72**, 115410 (2005); G. Weick, G.-L. Ingold, R. A. Jalabert, and D. Weinmann, *Phys. Rev. B* **74**, 165421 (2006); G. Weick, D. Weinmann, G.-L. Ingold, and R. A. Jalabert, *EPL* **78**, 27002 (2007).
  - [29] C. Seoanez, G. Weick, R. A. Jalabert, and D. Weinmann, *Eur. Phys. J. D* **44**, 351 (2007); G. Weick, G.-L. Ingold, D. Weinmann, and R. A. Jalabert, *Eur. Phys. J. D* **44**, 359 (2007).
  - [30] J. D. Jackson, *Classical Electrodynamics* (Wiley, New York, 1975).
  - [31] See Supplemental Material for a derivation of the CP dispersion from classical mechanics including the effect of dipole-dipole interaction beyond nearest neighbors, and for a derivation of the condition for having gapless plasmonic modes.
  - [32] N. W. Ashcroft and N. D. Mermin, *Solid State Physics* (Harcourt, Orlando, 1976).
  - [33] A. L. Fetter and J. D. Walecka, *Quantum Theory of Many-Particle Systems* (Dover, Mineola, 2003).
  - [34] J. Crowell and R. H. Smith, *Phys. Rev.* **172**, 436 (1968).
  - [35] C. Sönnichsen, T. Franzl, T. Wilk, G. von Plessen, J. Feldmann, O. Wilson, and P. Mulvaney, *Phys. Rev. Lett.* **88**, 077402 (2002).
  - [36] O. Hess, J. B. Pendry, S. A. Maier, R. F. Oulton, J. M. Hamm, and K. L. Tsakmakidis, *Nature Mater.* **11**, 573 (2012).
  - [37] J. Renger, R. Quidant, N. van Hulst, S. Palomba, and L. Novotny, *Phys. Rev. Lett.* **103**, 266802 (2009).